

RESPONSE TO EDITOR COMMENTS

TO MANUSCRIPT tc-2017-16-RC1

Title: Experimental observation of transient $\delta^{18}\text{O}$ interaction between snow and advective airflow under various temperature gradient conditions

Authors: Pirmin Philipp Ebner, Hans Christian Steen-Larsen, Martin Schneebeili, Barbara Stenni, and Aldo Steinfeld

We thank the Editor for his constructive comments and suggestions. All line numbers correspond to the annotated manuscript.

Comment The authors have responded well to both referees comments, and have made extensive revisions to their manuscript. I have identified only a couple of places where I think the manuscript needs attention. These should be easy to resolve before final publication.

Comment #1: There needs to be an explanation in the text for the identical density and porosity between experiment 1 and experiment 2. Even if the two specimens come from the same bulk sample, it would be surprising if they had the exact same density-- was the density measured on the bulk sample but not on the experimental specimens? In any case, if the density can only be determined to 5%, far too many significant precisions are included in table 1.

Revision: All snow samples were taken from the same snow block but the estimated porosity and density in Table 1 are the exact measured snow sample in each experiment by micro-CT. We reduced the number of decimals in Table 1 to a more realistic precision. We added a text in the methods part and in the caption of table 1.

“All snow samples were taken from the same snow block with an average density of $\approx 210 \text{ kg m}^{-3}$. The estimated density given in Table 1 was the density of the snow sample in each experiment measured by μCT .”

“Table 1: Morphological properties and flow characteristics of the experimental runs: μCT measured snow density (ρ), porosity (ϵ), specific surface area per unit mass (SSA), mean pore space diameter (d_{mean}), ...”

Comment #2: The wording of the revision in response to R1's comment 18 is a bit confusing: I would recommend writing: "The mean pore size distribution(d_{mean}) was estimated using the opening-size-distribution operation. This operation can be imagined..."

Revision: Text changed in the revised manuscript.

Comment #3: The revision in response to R1's comment 23 is not clear. I think there are some words missing from the second sentence, and the authors need to be clear whether the memory effect is known to have been important, or whether it is one possible effect that might have produced the observer result.

Revision: We changed this part and added a reference that the memory effect is known but not relevant for the results.

“In the first approximately 30 min, the isotopic composition of the measured outflow air $\delta^{18}\text{O}$ increased from a low $\delta^{18}\text{O}$ to a starting value of around -29‰ in each experiment. This was due to memory effect and one possible effect might be condensed water left in the tubes from a prior experiment which had no further impact on the experiments (Penna et al., 2012).”.

Reference added:

Penna, D., Stenni, B., Šanda, M., Wrede, S., Bogaard, T. A., Michelini, M., et al. (2012). Technical Note: Evaluation of between-sample memory effects in the analysis of $\delta^2\text{H}$ and $\delta^{18}\text{O}$ of water samples measured by laser spectrometers. *Hydrology and Earth System Sciences*, 16(10), 3925–3933. <http://doi.org/10.5194/hess-16-3925-2012>.

Comment #4: At line 196 of the annotated manuscript, there's a sentence that begins "In wind pumping theory..." I'd recommend rewriting this sentence in the active voice to make clear who used the wind-pumping theory, and then make clear whether your calculation of Re also uses the same wind-pumping theory.

Revision: Text changed in the revised manuscript.

“We performed the experiments with airflow velocities in the snow sample at $u_D \approx 30 \text{ mm s}^{-1}$, which is a factor of three higher than calculated by Neumann (2003) for a natural snow pack. But looking at the Reynolds number, describing the flow regime inside the pores, our experiments ($Re \approx 0.7$) were in the feasible flow regime (laminar flow) of a natural snow pack ($Re \approx 0.65$).”

Minor revisions were made throughout the revised manuscript.

We thank the Editor for his insight, suggestions and recommendations.

The authors

1 Experimental observation of transient $\delta^{18}\text{O}$ interaction between snow and
2 advective airflow under various temperature gradient conditions

3
4 Pirmin Philipp Ebner¹, Hans Christian Steen-Larsen^{2,3}, Barbara Stenni⁴, Martin
5 Schneebeli^{1,*}, and Aldo Steinfeld⁵

6 ¹ *WSL Institute for Snow and Avalanche Research SLF, 7260 Davos Dorf, Switzerland*

7 ² *LSCE Laboratoire des Sciences du Climat et de l'Environnement, Gif-Sur-Yvette Cedex, France*

8 ³ *Center for Ice and Climate, Niels Bohr Institute, University of Copenhagen, Copenhagen, Denmark*

9 ⁴ *Department of Environmental Sciences, Informatics and Statistics, University Ca' Foscari of Venice,*
10 *Venice, Italy*

11 ⁵ *Department of Mechanical and Process Engineering, ETH Zurich, 8092 Zurich, Switzerland*

12
13 **Abstract**

14 Stable water isotopes ($\delta^{18}\text{O}$) obtained from snow and ice samples of polar regions
15 are used to reconstruct past climate variability, but heat and mass transport processes
16 can affect the isotopic composition. Here we present an experimental study on the effect
17 of airflow on the snow isotopic composition through a snow pack in controlled
18 laboratory conditions. The influence of isothermal and controlled temperature gradient
19 conditions on the $\delta^{18}\text{O}$ content in the snow and interstitial water vapor is elucidated. The
20 observed disequilibrium between snow and vapor isotopes led to the exchange of
21 isotopes between snow and vapor under non-equilibrium processes, significantly
22 changing the $\delta^{18}\text{O}$ content of the snow. The type of metamorphism of the snow had a
23 significant influence on this process. These findings are pertinent to the interpretation of
24 the records of stable isotopes of water from ice cores. These laboratory measurements

* Corresponding author. Email: schneebeli@slf.ch

25 suggest that a highly resolved climate history is relevant for the interpretation of the
26 snow isotopic composition in the field.

27

28 *Keywords:* snow, isotope, isothermal, metamorphism, advection, tomography, post-depositional process

29

30 **1. Introduction**

31 Water stable isotopes in polar snow and ice have been used for several decades as
32 proxies for global and local temperatures (e.g. Dansgaard, 1964; Lorius et al., 1979;
33 Grootes et al., 1994; Petit et al., 1999; Johnsen et al., 2001; EPICA Members, 2004).
34 However, the processes that influence the isotopic composition of precipitation in high-
35 latitude are complex, making direct inference of paleo temperatures from the isotopic
36 record difficult (Cuffey et al., 1994; Jouzel et al., 1997, 2003; Hendricks et al., 2000).
37 Several factors affect the vapor and snow isotopic composition, which give rise to ice
38 core isotopic composition, starting from the process of evaporation in the source region,
39 transportation of the air mass to the top of the ice sheet, and post-depositional processes
40 (Craig and Gordon, 1964; Merlivat and Jouzel, 1979; Johnsen et al. 2001; Ciais and
41 Jouzel, 1994; Jouzel and Merlivat, 1984; Jouzel et al., 2003; Helsen et al., 2005, 2006,
42 2007; Cuffey and Steig, 1998; Krinner and Werner, 2003). Mechanical processes such
43 as mixing, seasonal scouring, or spatial redistribution of snow can alter seasonal and
44 annual records (Fisher et al., 1983; Hoshina et al., 2014). Post-depositional processes
45 associated with wind scouring and snow redistribution are known to introduce a “post-
46 depositional noise” in the surface snow. Comparisons of isotopic records obtained from
47 closely located shallow ice cores have allowed for estimation of a signal-to-noise ratio

48 and a common climate signal (Fisher and Koerner, 1988, 1994; White et al., 1997;
49 Steen-Larsen et al., 2011; Sjolte et al., 2011; Masson-Delmotte et al., 2015). After
50 deposition, interstitial diffusion in the firn and ice affects the water-isotopic signal but
51 back-diffusion or deconvolution techniques have been used to establish the original
52 isotope signal (Johnsen, 1977; Johnsen et al., 2000).

53 Snow is a bi-continuous material consisting of fully connected ice crystals and pore
54 space (air) (Löwe et al., 2011). Because of the proximity to the melting point, the high
55 vapor pressure causes a continuous recrystallization of the snow microstructure known
56 as snow metamorphism, even under moderate temperature gradients (Pinzer et al.,
57 2012). The whole ice matrix is continuously recrystallizing by sublimation and
58 deposition, with vapor diffusion as the dominant transport process. Pinzer et al. (2012)
59 showed that a typical half-life of the ice matrix is a few days. The intensity of the
60 recrystallization is dictated by the temperature gradient and this can occur under mid-
61 latitude or polar conditions. Temperature, and geometrical factors (porosity and specific
62 surface area) also play a significant role (Pinzer and Schneebeli, 2009; Pinzer et al.,
63 2012).

64 The interpretation of ice core data and the comparison with atmospheric model
65 results implicitly rely on the assumption that the snowfall precipitation signal is
66 preserved in the snow-ice matrix (Werner et al., 2011). Classically, ice-core stable-
67 isotope records are interpreted as reflecting precipitation-weighted signals, and
68 compared to observations and atmospheric model results for precipitation, ignoring
69 snow-vapor exchanges between surface snow and atmospheric water vapor (e.g. Persson
70 et al., 2011). However, recent studies carried out on top of the Greenland and Antarctic
71 ice sheets combining continuous atmospheric water vapor isotope observations with
72 daily snow surface sampling document a clear day-to-day variation of isotopic

73 composition of surface snow between precipitation events as well as diurnal change in
74 the snow isotopes (Steen-Larsen et al., 2014a; Ritter et al., 2016; Casado et al., 2016).
75 This effect was interpreted as being caused by the uptake of the synoptic-driven
76 atmospheric water-vapor isotope signal by individual snow crystals undergoing snow
77 metamorphism (Steen-Larsen et al., 2014a) and the diurnal variation in moisture flux
78 (Ritter et al., 2016). However, the impact of this process on the isotope-temperature
79 reconstruction is not yet sufficiently understood, but crucial to constrain. This process,
80 compared to interstitial diffusion (Johnsen, 1977; Johnsen et al., 2000), will alter the
81 isotope mean value. The field observations challenge the previous assumption that
82 sublimation occurred molecular layer-by-layer with no resulting isotopic fractionation
83 (Dansgaard, 1964; Friedman et al., 1991; Town et al., 2008; Neumann and Waddington,
84 2004). It is assumed that the solid undergoing sublimation would not be unduly enriched
85 in the heavier isotope species due to the preferential loss of lighter isotopic species to
86 the vapor (Dansgaard, 1964; Friedman et al., 1991). Because self-diffusion in the ice is
87 about three orders of magnitude slower than molecular diffusion in the vapor, the
88 amount of isotopic separation in snow is assumed to be negligible.

89 Snow has a high permeability (Calonne et al., 2012; Zermatten et al., 2014), which
90 facilitates diffusion of gases and, under appropriate conditions, airflow (Gjessing, 1977;
91 Colbeck, 1989; Sturm and Johnson, 1991; Waddington et al., 1996). In a typical
92 Antarctic and Greenland snow profile, strong interactions between the atmosphere and
93 snow occurs, especially in the first 2 m (Neumann and Waddington, 2004; Town et al.,
94 2008), called the convective zone. In the convective zone, air can move relatively freely
95 and therefore exchange between snow and the atmospheric air occurs. Air flowing into
96 the snow reaches saturation vapor pressure nearly instantly through sublimation
97 (Neumann et al., 2008; Ebner et al., 2015a). Models of the influence of the so-called

98 ‘wind pumping’-effect (Fisher et al., 1983; Neumann and Waddington, 2004), in which
99 the interstitial water vapor is replaced by atmospheric air pushed through the upper
100 meters of the snow pack by small-scale high and low pressure areas caused by irregular
101 grooves or ridges formed on the snow surface (dunes and sastrugi), have assumed that
102 the snow grains would equilibrate with the interstitial water vapor on timescales
103 governed by ice self-diffusion. However, no experimental data are available to support
104 this assumption. With this in mind the experimental study presented here is specifically
105 developed to investigate the effect of ventilation inside the snow pack on the isotopic
106 composition. Only conditions deeper than 1 cm inside a snowpack are considered.
107 Previous work showed that (1) under isothermal conditions, the Kelvin effect leads to a
108 saturation of the pore space in the snow but does not affect the structural change (Ebner
109 et al., 2015a); (2) applying a negative temperature gradient along the flow direction
110 leads to a change in the microstructure due to deposition of water molecules on the ice
111 matrix (Ebner et al., 2015b); and (3) a positive temperature gradient along the flow had
112 a negligible total mass change of the ice but a strong reposition effect of water
113 molecules on the ice grains (Ebner et al., 2016). Here, we continuously measured the
114 isotopic composition of an airflow containing water vapor through a snow sample under
115 both isothermal and temperature gradient conditions. Micro computed-tomography
116 (μ CT) was applied to obtain the 3D microstructure and morphological properties of
117 snow.

118 **2. Experimental setup**

119 Isothermal and temperature gradient experiments with fully saturated airflow and
120 defined isotopic composition were performed in a cold laboratory at around $T_{\text{lab}} \approx -15$
121 °C with small fluctuations of ± 0.8 °C (Ebner et al., 2014). Snow produced from de-
122 ionized tap water in a cold laboratory (water temperature: 30 °C; air temperature: -20

123 °C) was used for the snow sample preparation (Schleef et al., 2014). The snow was
124 sieved with a mesh size of 1.4 mm into a box, and isothermally sintered for 27 days at -
125 5 °C to increase the strength, in order to prevent destruction of the snow sample due to
126 the airflow, and to evaluate the effect of metamorphism of snow. The morphological
127 properties of the snow are listed in Table 1. The sample holder (diameter 53 mm, height
128 30 mm, 0.066 liter) was filled by a cylinder cut out from the sintered snow. To prevent
129 air flow between snow sample and the sample holder walls, the undisturbed snow disk
130 was filled in at a higher temperature (about -5 °C) and sintering was allowed for about 1
131 h before cooling down and start of the experiment. The setup of Ebner et al. (2014) was
132 modified by additionally inserting a water vapor isotope analyzer (Model: L1102-I
133 Picarro, Inc., Santa Clara, CA, USA) to measure the isotopic ratio $\delta^{18}\text{O}$ of the water
134 vapor contained in the airflow at the inlet and outlet of the sample holder. The
135 experimental setup consisted of three main components (humidifier, sample holder, and
136 the Picarro analyzer) connected with insulated copper tubing and Swagelok fitting (Fig.
137 1). The tubes to the Picarro analyzer were heated to prevent deposition of water vapor
138 and thereby fractionation. The temperature was monitored with thermistors inside the
139 humidifier and at the inlet and outlet of the snow sample. A dry air pressure tank
140 controlled by a mass flow controller (EL-Flow, Bronkhorst) generated the airflow. A
141 humidifier, consisting of a tube (diameter 60 mm, height 150 mm, 0.424 liter volume)
142 filled with crushed ice particles (snow from Antarctica with low $\delta^{18}\text{O}$ composition), was
143 used to saturate the dry air entering the humidifier with water vapor at an almost
144 constant isotopic composition. The air temperature in the humidifier and at the inlet of
145 the snow sample was maintained at the same value (accuracy ± 0.2 K) to limit the
146 influence of variability in absolute vapor pressure and isotopic composition. We
147 measured the $\delta^{18}\text{O}$ of the water vapor produced by the humidifier before and after each

148 experimental run ($\delta^{18}\text{O}_{\text{hum}}$). The outlet flow ($\delta^{18}\text{O}_a$) of the sample holder was
149 continuously measured during the experiment to analyze the temporal evolution of the
150 isotopic signal. All data from the Picarro analyzer were corrected to the humidity
151 reference level using the established instrument humidity-isotope response (Steen-
152 Larsen et al. 2013; 2014b). In addition, VSMOW-SLAP correction and drift correction
153 were performed. We followed the calibration protocol and used the calibration system
154 described in detail by Steen-Larsen et al. (2013; 2014b).

155 The sample holder described by Ebner et al. (2014) was used to analyze the snow by
156 μCT . Tomography measurements were performed with a modified $\mu\text{-CT80}$ (Scanco
157 Medical). The equipment incorporated a microfocus X-ray source, operated at 70 kV
158 acceleration voltage with a nominal resolution of 18 μm . The samples were scanned
159 with 1000 projections per 180° in high-resolution setting, with typical adjustable
160 integration time of 200 ms per projection. The field of view of the scan area was 36.9
161 mm of the total 53 mm diameter, and subsamples with a dimension of $7.2 \times 7.2 \times 7.2$
162 mm^3 were extracted for further processing. The reconstructed μCT images were filtered
163 using a $3 \times 3 \times 3$ median filter followed by a Gaussian filter ($\sigma = 1.4$, support = 3). The
164 Otsu method (Otsu, 1979) was used to automatically perform clustering-based image
165 thresholding to segment the grey-level images into ice and void phase. Morphological
166 properties in the two-phase system were determined based on the exact geometry
167 obtained by the μCT . Tetrahedrons corresponding to the enclosed volume of the
168 triangulated ice matrix surface were applied on the segmented data to determine
169 porosity (ε) and specific surface area (SSA). ~~Opening-size-distribution-operation-was~~
170 ~~applied-in-the-segmented- μCT -data-to-extract-the-mean-pore-size- (d_{mean}) .~~ The mean pore
171 size distribution was estimated using the opening-size-distribution operation. This

172 operation can be ~~The opening size distribution can be~~ imagined as virtual sieving with
173 different mesh size (Haussener et al., 2012).

174 Three experiments with saturated advective airflow through the snow sample were
175 performed to record the following parameters and analyze their effects: (1) isothermal
176 conditions to analyze the influence of curvature effects (Kaempfer al et., 2007); (2)
177 positive temperature gradient applied to the snow sample where cold air entering the
178 sample is heated while flowing through the sample in order to analyze the influence of
179 sublimation; (3) negative temperature gradient applied to the snow sample where warm
180 air entering the sample is cooled while flowing across the sample, to analyze the
181 influence of net deposition. During the temperature gradient experiments, a temperature
182 difference of 1.4 °C and 1.8 °C was imposed resulting in a gradient of +47 K m⁻¹ and -60
183 K m⁻¹, respectively. The runs were performed at atmospheric pressure and with a
184 volume flow rate of 3.0 liter min⁻¹ corresponding to an average flow speed in the pores
185 of $u_D \approx 30 \text{ mm s}^{-1}$. ~~We performed the experiments with airflow velocities in the snow~~
186 ~~sample at $u_D \approx 30 \text{ mm s}^{-1}$, which is a factor of three higher than calculated by Neumann~~
187 ~~(2003) for a natural snow pack. But looking at the Reynolds number, describing the~~
188 ~~flow regime inside the pores, our experiments ($Re \approx 0.7$) were in the feasible flow~~
189 ~~regime (laminar flow) of a natural snow pack ($Re \approx 0.65$). In wind pumping theory, an~~
190 ~~airflow velocity of $u_D \approx 10 \text{ mm s}^{-1}$ (corresponding Reynolds number $Re \approx 0.65$) was~~
191 ~~estimated inside the surface snow layers ($d_{\text{mean}} \approx 1 \text{ mm}$) for a high wind speed above the~~
192 ~~snow surface ($\sim 10 \text{ m s}^{-1}$) (Neumann, 2003). We performed experiments with airflow~~
193 ~~velocities inside the snow sample of around 30 mm s^{-1} (corresponding Reynolds number~~
194 ~~$Re = 0.7$), which was a factor three higher than in natural conditions. But looking at the~~
195 ~~Reynolds number our experiments were in the feasible flow regime (laminar flow) of a~~
196 ~~natural snow pack.~~ In experiment (2) the outlet temperature and in experiment (3) the

197 inlet and also the humidifier temperature were actively controlled using thermo-electric
198 elements. Variations in temperature of up to ± 0.8 °C were due to temperature
199 fluctuations inside the cold laboratory, leading to slightly variable temperature gradients
200 and mean temperature in experiment (2) and (3). Table 1 presents a summary of the
201 experimental conditions and the morphological properties of the snow samples. All
202 snow samples were taken from the same snow block with an average density of ≈ 210
203 kg m^{-3} . The density given in Table 1 was the density of the snow sample in each
204 experiment measured by μCT . At the end of each experiment, the snow sample was cut
205 into five layers of 6 mm height and the isotopic composition of each layer was analyzed
206 to examine the spatial $\delta^{18}\text{O}$ gradient in the isotopic composition of the snow sample.

207 A slight increase with a maximum of 0.7 ‰ of $\delta^{18}\text{O}$ in the water vapor produced by
208 the humidifier was observed in experiment (1), with lower increases during experiments
209 (2) and (3) (Table 2). This change of $\sim 0.7\text{‰}$ is not significant compared to the
210 difference between the isotopic composition of the water vapor and the snow sample in
211 the sample holder of $\sim 53\text{‰}$ and the temporal change of the water vapor isotopes on the
212 back side of the snow sample.

213 In the first approximately 30 min, the isotopic composition of the measured outflow
214 air $\delta^{18}\text{O}_a$ increased from a low $\delta^{18}\text{O}$ to a starting value of around -29‰ in each
215 experiment. This was due to memory effect and one possible effect might be condensed
216 water left in the tubes from a prior experiment which had no further impact on the
217 experiments (Penna et al., 2012). ~~This was due to memory effect possible condensed~~
218 ~~water left in the tubes from a prior experiment.~~

219 **3. Results**

220 **3.1 Isothermal condition**

221 The experiment (1) was performed for 24 h at a mean temperature of $T_{\text{mean}} = -15.5$
222 °C. $\delta^{18}\text{O}_a$ decreased exponentially in the outlet flow observed throughout the
223 experimental run as shown in Fig. 2. Initially, the $\delta^{18}\text{O}_a$ content in the flow was -27.7‰
224 and exponentially decreased to -47.6‰ after 24 h. The small fluctuations in the $\delta^{18}\text{O}_a$
225 signal at $t \approx 7$ h, 17 h and 23 h were due to small temperature changes in the cold
226 laboratory.

227 We observed a strong interaction between the airflow and the snow as manifest by
228 the isotopic composition of the snow. The $\delta^{18}\text{O}_s$ signal in the snow decreased by $4.75 -$
229 7.78‰ and an isotopic gradient in the snow was observed after the experimental run,
230 shown in Fig. 3. Initially, the snow had a homogeneous isotopic composition of $\delta^{18}\text{O}_s =$
231 -10.97‰ but post-experiment sampling showed a decrease in the snow $\delta^{18}\text{O}$ at the inlet
232 side to -17.75‰ and at the outlet side to -15.72‰ . The spatial $\delta^{18}\text{O}_s$ gradient of the
233 snow had an approximate slope of 0.68‰ mm^{-1} at the end of the experimental run.
234 Table 2 shows the $\delta^{18}\text{O}$ value in snow at the beginning ($t = 0$) and end ($t = 24$ h) of the
235 experiment.

236 **3.2 Air warming by a positive temperature gradient along the airflow**

237 The experiment (2) was performed over a period of 24 h with an average
238 temperature gradient of approximately $+47\text{ K m}^{-1}$ (warmer temperatures at the outlet
239 of the snow) and an average mean temperature of -14.7 °C . As in the isothermal
240 experiment (1), we observed a relaxing exponential decrease of $\delta^{18}\text{O}_a$ in the outlet flow
241 throughout the measurement period as shown in Fig. 2, but the decrease was slower
242 compared to the isothermal run. Initially, the $\delta^{18}\text{O}_a$ content in the flow coming through
243 the snow disk was -29.8‰ and exponentially decreased to -41.9‰ after 24 h. The
244 small fluctuations in the $\delta^{18}\text{O}_a$ signal at $t \approx 2.7$ h, and 12.7 h were due to small
245 temperature changes in the cold laboratory.

246 The $\delta^{18}\text{O}_s$ signal in the snow decreased 4.66 – 7.66 ‰ and a gradient in the isotopic
247 composition of the snow was observed after the experimental run, shown in Fig. 3.
248 Initially, the snow had a homogeneous isotopic composition of $\delta^{18}\text{O}_s = -11.94$ ‰, but
249 post-experiment sampling showed a decrease at the inlet side to -19.6 ‰ and at the
250 outlet side to -16.6 ‰. The spatial $\delta^{18}\text{O}_s$ gradient of the snow had an approximate slope
251 of 1.0 ‰ mm^{-1} at the end of the experimental run. Table 2 shows the $\delta^{18}\text{O}_s$ value in
252 snow at the beginning ($t = 0$) and end ($t = 24$ h) of the experiment.

253 **3.3 Air cooling by a negative temperature gradient along the air flow**

254 The experiment (3) was performed for 84 h instead of 24 h to better estimate the
255 trend in $\delta^{18}\text{O}_a$ in the outlet flow. An average temperature gradient of approximately -60
256 K m^{-1} (colder temperatures at the outlet of the snow) and an average mean temperature
257 of -13.2 °C were observed during the experiment. As in the previous experiments, a
258 relaxing exponential decrease of $\delta^{18}\text{O}_a$ in the outlet flow was observed throughout the
259 experimental run as shown in Fig. 2, but the decrease was slower compared to the
260 isothermal run and temperature gradient opposed to the airflow. Initially, the $\delta^{18}\text{O}_a$
261 content in the flow was -29.8 ‰ and exponentially decreased to -37.7 ‰ after 84 h. The
262 small fluctuations in the $\delta^{18}\text{O}_a$ signal at $t \approx 7.3$ h, 21.3 h, 31.3 h, 45.3 h, 55.3 h, 69.3 h,
263 and 79.3 h were due to small temperature changes in the cold laboratory.

264 The $\delta^{18}\text{O}_s$ signal in the snow decreased 4.46 – 15.09 ‰ and a gradient in the isotopic
265 composition of the snow was observed after the experimental run, shown in Fig. 3.
266 Initially, the snow had an isotopic composition of $\delta^{18}\text{O}_s = -10.44$ ‰ but post-experiment
267 sampling showed a decrease at the inlet side to -25.53 ‰ and at the outlet side to -15.00
268 ‰. The spatial $\delta^{18}\text{O}_s$ gradient of the snow had an approximate slope of 3.5 ‰ mm^{-1} at
269 the end of the experimental run. Table 2 shows the $\delta^{18}\text{O}_s$ value in snow at the beginning
270 ($t = 0$) and end ($t = 84$ h) of the experiment.

271 4. Discussion

272 All experiments showed a strong exchange in $\delta^{18}\text{O}$ between the snow and water-
273 vapor saturated air resulting in a significant change of the value of the stable isotopes in
274 the snow. The advective conditions in the experiments were comparable with surface
275 snow layers in Antarctica and Greenland, but at higher temperature, especially
276 compared to interior Antarctica.

277 The results also showed strong interactions in $\delta^{18}\text{O}$ between snow and air depending
278 on the different temperature gradient conditions. The experiments indicate that
279 temperature variation and airflow above and through the snow structures (Sturm and
280 Johnson, 1991; Colbeck, 1989; Albert and Hardy, 1995) seem to be dominant processes
281 affecting water stable isotopes of surface snow. The results also support the statement
282 that an interplay between theoretically expected layer-by-layer sublimation and
283 deposition at the ice-matrix surface and the isotopic content evolution of snow cover
284 due to mass exchange between the snow cover and the atmosphere occurs (Sokratov and
285 Golubev, 2009). The specific surface area of snow exposed to mass exchange (Horita et
286 al., 2008) and by the depth of the snow layer exposed to the mass exchange with the
287 atmosphere (He and Smith, 1999) plays an important role. Our results support the
288 interpretation that changes in surface snow isotopic composition are expected to be
289 significant if large day-to-day surface changes in water vapor occur in between
290 precipitation events, wind pumping is efficient and snow metamorphism is enhanced by
291 temperature gradients in the upper first centimeters of the snow (Steen-Larsen et al.,
292 2014a).

293 We expect that our findings will lead to improvement of the interpretation of the
294 water stable isotope records from ice cores. Classically, ice core stable isotope records
295 are interpreted as paleo-temperature reflecting precipitation-weighted signals. When

296 comparing observations and atmospheric model results for precipitation with ice core
297 records, such vapor-snow exchanges are normally ignored (e.g. Persson et al., 2011;
298 Fujita and Abe, 2006). However, vapor-snow exchange enhanced by recrystallization
299 rate seems to be an important factor for the high variation in the snow surface $\delta^{18}\text{O}$
300 signal as supported by our experiments. It was hypothesized that the changes in the
301 snow-surface $\delta^{18}\text{O}$ reported by Steen-Larsen et al. (2014a) are caused by changes in
302 large-scale wind and moisture advection of the atmospheric water vapor signal and
303 snow metamorphism. The strong interaction between atmosphere and near-surface snow
304 can modify the ice core water stable isotope records.

305 The rate-limiting step for isotopic exchange in the snow is isotopic equilibration
306 between the pore-space vapor and surrounding ice grains. The relaxing exponential
307 decrease of $\delta^{18}\text{O}$ in the outflow of our experiments predicted that full isotopic
308 equilibrium between snow and atmospheric vapor will not be reached at any depth
309 (Waddington et al., 2002; Neumann and Waddington, 2004) but changes towards
310 equilibrium with the atmospheric state occurs (Steen-Larsen et al., 2013, 2014a).

311 As snow accumulates, the upper 2 m are advected through the ventilated zone
312 (Neumann and Waddington, 2004; Town et al., 2008). In areas with high accumulation
313 rate (e.g. South Greenland), snow is advected for a short time through the ventilated
314 zone. The snow exposed a relatively short time to vapor snow exchange would result in
315 higher spatial variability compared to long-time exposure. However, the effects of snow
316 ventilation on isotopic composition may become more important as the accumulation
317 rate of the snow decreases ($< 50 \text{ mm a}^{-1}$), such that snow remains in the near-surface
318 ventilated zone for many years (Waddington et al., 2002; Hoshina et al., 2014; Hoshina
319 et al., 2016). As the snow remains longer in the near-surface ventilated zone, a larger
320 $\delta^{18}\text{O}$ exchange between snow and atmospheric vapor will occur. Consequently, the

321 isotopic content of layers at sites with high and low accumulation rates can evolve
322 differently, even if the initial snow composition had been equal, and the sites had been
323 subjected to the same histories of air-mass vapor.

324 Despite a relatively small change in the difference between the isotopic composition
325 of the incoming vapor and the snow, large differences in the isotopic composition of the
326 water vapor at the outlet flow exist for the three different experimental setups. Based on
327 the difference in the outlet water vapor isotopic composition, we hypothesized that
328 different processes are at play for the different experiments. It is obvious that there is a
329 fast isotopic exchange with the surface of the ice crystals, and a much slower timescale
330 on which the interior of the ice crystals is altered. Due to the low diffusivity of H_2^{16}O
331 and H_2^{18}O in ice ($D_{\text{H}_2^{18}\text{O}} \approx D_{\text{H}_2^{16}\text{O}} = \sim 10^{-15} \text{ m}^2 \text{ s}^{-1}$ (Ramseier, 1967; Johnsen et al., 2000),
332 we assumed that the interior of the ice crystals is not altered on the timescale of the
333 experiment. This explained why the net isotopic change of the bulk sample is relatively
334 small compared to the changes in the outlet water vapor isotopes. The effective ‘ice-
335 diffusion depth’ of the isotopic exchange during the experiments is given as $L_D = \sqrt{D \cdot t}$,
336 where D is the diffusion coefficient of H_2^{16}O and H_2^{18}O in ice, respectively, and t the
337 experimental time. The calculated ‘ice-diffusion depth’ L_D , is $\sim 9.3 \mu\text{m}$ for experiments
338 (1) and (2), and $\sim 17.4 \mu\text{m}$ for experiment (3), respectively, indicating an expected a
339 minimal change of the interior of the ice crystal. However, snow has a large specific
340 surface area and therefore a high exchange area. This has an effect on the $\delta^{18}\text{O}$ snow
341 concentration. The fraction of the total volume V_{tot} of ice that is close enough to the ice
342 surface to be affected by diffusion in time t is then $\rho_{\text{ice}} \cdot \text{SSA} \cdot L_D$, where SSA is the
343 specific surface area (area per unit mass), and L_D is the diffusion depth, defined above,
344 for time t . For $t \approx 24$ hours, a large fraction (24 to 43 %) of the total volume V_{tot} of the
345 ice matrix can be accessed through diffusion. It is quite hard to see the total $\delta^{18}\text{O}$ snow

346 difference between experiments (1) and (2) after the experiment compared to the $\delta^{18}\text{O}$
347 of the vapor in the air at the outlet. There is a small, but notable, difference in the total
348 $\delta^{18}\text{O}$ of the snow between experiment (1) and (2). Due to the higher recrystallization
349 rate of experiment (2) the spatial $\delta^{18}\text{O}_s$ gradient of the snow (1.0‰ mm^{-1}) is higher than
350 for experiment (1) (0.68‰ mm^{-1}). Increasing the experimental time, the $\delta^{18}\text{O}$ change in
351 the snow increases (experiment (3)). In general, the calculated ‘ice-diffusion depth’ is
352 realistic under isothermal conditions where diffusion processes are the main factors
353 (Kaempfer and Schneebeli, 2007; Ebner et al., 2015). Applying a temperature gradient,
354 the impact of diffusion is suppressed due to the high recrystallization rate by
355 sublimation and deposition. Due to the low half-life of the ice matrix of a few days, the
356 growth rates are typically on the order of $100\text{ }\mu\text{m}$ per day (Pinzer et al., 2012).
357 Therefore, this redistribution of ice caused by temperature gradient counteracts the
358 diffusion into the solid ice.

359 By comparing similarities and differences between the outcomes of the three
360 experimental setups we will now discuss the physical processes influencing the
361 interaction and exchange processes within the snowpack between the snow and the
362 advected vapor. We first notice that the final snow isotopic profile of experiment (1)
363 (isothermal) and (2) (positive temperature gradient along the direction of the flow) are
364 comparable to each other. Despite this similarity, the evolution in the outlet water vapor
365 of experiment (1) showed a significantly stronger depletion compared to experiment (2).
366 For experiment (3) (negative temperature gradient along the direction of the flow) we
367 observed the smallest change in outlet water vapor isotopes but the largest snow-pack
368 isotope gradient after the experiment. However, this change was caused by 84 hours
369 flow instead of 24 hours.

370 Curvature effects, temperature gradients and therefore the recrystallization rate
371 influence the mass transfer of $\text{H}_2^{16}\text{O}/\text{H}_2^{18}\text{O}$ molecules. The higher the recrystallization
372 rate of the snow the slower the adaption of the outlet air concentration to the inlet air
373 concentration (see in experiment (2) and (3)). Under isothermal conditions (experiment
374 (1)) the only effect influencing the recrystallization rate is the curvature effect
375 (Kaempfer and Schneebeli, 2007). However, based on the experimental observations
376 (Kaempfer and Schneebeli, 2007) this effect decreases with decreasing temperature and
377 increasing experimental time. Applying an additional temperature gradient on a snow
378 sample causes complex interplays between local sublimation and deposition on surfaces
379 and the interaction of water molecules in the air with the ice matrix due to changing
380 saturation conditions of the airflow. Therefore, the recrystallization rate increases and
381 causes the change in the $\delta^{18}\text{O}$ of the air. For experiment (2) there is a complex interplay
382 between sublimation and deposition of water molecules into the interstitial flow (Ebner
383 et al., 2015c) while for experiment (3) there is deposition of molecules carried by the
384 interstitial flow onto the snow crystals (Ebner et al., 2015b). Furthermore, in the
385 beginning of each experiment there is a tendency to sublimate from edges of the
386 individual snow crystals due to the higher curvature. As the edges were sublimated and
387 deposition occurred in the concavities, the individual snow crystals became more
388 rounded, slowing down the transfer of water molecules into the interstitial airflow. We
389 noticed for all three experiments that within the uncertainty of the isotopic composition
390 of the snow, the initial isotopic composition of the vapor was the same and in isotopic
391 equilibrium with the snow. The difference between experiment (1) and (2) lies in the
392 fact that due to the temperature gradient in experiment (2) there is an increased transfer
393 of water vapor with the isotopic composition of the snow into the airflow. Hence the
394 depleted air from the humidifier advected through the snow disk is mixed with a

395 relatively larger vapor flux from the snow crystals. Additionally, we also expected less
396 deposition into the concavities in experiment (2) compared to experiment (1). However,
397 it is interesting to note that the final isotopic profile of the snow disk is similar in
398 experiment (1) and experiment (2). We interpreted this as being a result of two
399 processes acting in opposite direction: although relatively isotope-depleted vapor from
400 the humidifier was deposited on the ice matrix there was also a higher amount of
401 sublimation of relatively isotope-enriched vapor from the snow disk in experiment (2).
402 Experiment (3) separates itself from the other two experiments in the way that as the
403 water vapor from the humidifier is advected through the snow disk there is a continuous
404 deposition of very depleted air due the negative temperature gradient. As for the case of
405 experiment (1) and (2) there was also in experiment (3) a constant sublimation of the
406 convexities into the vapor stream. We notice that despite the fact that experiment (3) ran
407 for 84 hours the snow at the outlet side of the snow-disk did not become more
408 isotopically depleted compared to experiment (1) and (2). However, the snow on the
409 inlet side became significantly more isotopically depleted. This observation, together
410 with the fact that the vapor of the outlet of the snow-disk is less depleted compared to
411 experiment (1) and (2), leads us to hypothesize that there is a relatively larger deposition
412 of isotopically depleted vapor from the humidifier as the vapor is advected through the
413 snow disk. This means that a relatively larger component of the isotopic composition of
414 the vapor is originating by sublimation from the convexities of the snow disk and less
415 from the isotopically depleted vapor from the humidifier.

416 Our results and conclusions indicate that there is a need for additional validation.
417 Specifically, it would be crucial to know the mass balance of the snow disk more
418 precisely, which could be done by reconstructing the entire snow disk following the
419 change in density and morphological properties over the entire height. Ideally, the entire

420 sample would be tomographically measured with a resolution of $4 \times 4 \times 4 \text{ mm}^3$, each
421 cube corresponding to the representative volume. Insights would also be achieved with
422 experiments using snow of the same isotopic composition, but different SSA, as more
423 precise calculation of the different observed exchange rates would be allowed.
424 Additionally, different and colder background temperatures should be tested to better
425 understand inland Antarctic environment and the effect of the quasi-liquid layer, which
426 is necessary for the development of a numerical model. Isotopically different
427 combinations of vapor and snow should be performed. In the present manuscript, vapor
428 with low $\delta^{18}\text{O}$ isotopic composition was transported through snow with relative high
429 $\delta^{18}\text{O}$ isotopic composition. It would be interesting to reverse the combination and
430 perform experiments with different combinations to provide more insights on mass and
431 isotope exchanges between vapor and snow. Experiments with longer running time help
432 to understand the change in the ice matrix better under low accumulation conditions.

433 **4. Summary and conclusion**

434 Laboratory experimental runs were performed where a transient $\delta^{18}\text{O}$ interaction
435 between snow and air was observed. The airflow altered the isotopic composition of the
436 snowpack and supports an improved climatic interpretation of ice core stable water
437 isotope records. The water vapor saturated airflow with an isotopic difference of up to
438 55‰ changed within 24 h and 84 h the original $\delta^{18}\text{O}$ isotope signal in the snow by up to
439 7.64 ‰ and 15.06 ‰. The disequilibrium between snow and air isotopes led to the
440 observed exchange of isotopes, the rate depending on the temperature gradient
441 conditions. Concluding, increasing the recrystallization rate in the ice matrix causes the
442 temporal change of the $\delta^{18}\text{O}$ concentration at the outflow to decrease (experiment (2)
443 and (3)). Decreasing the recrystallization rate causes the temporal curve of the outlet

444 concentration to become steeper reaching the $\delta^{18}\text{O}$ inlet concentration of the air faster
445 (experiment (1)).

446 Additionally, the complex interplay of simultaneous diffusion, sublimation and
447 deposition due to the geometrical complexity of snow has a strong effect on the $\delta^{18}\text{O}$
448 signal in the snow and cannot be neglected. A temporal signal can be superimposed on
449 the precipitation signal, (a) if the snow remains near the surface for a long time, i.e. in a
450 low-accumulation area, and (b) is exposed to a history of air masses carrying vapor with
451 a significantly different isotopic signature than the precipitated snow.

452 These are novel measurements and will therefore be important as the basis for
453 further research and experiments. Our results represent direct experimental observation
454 of the interaction between the water isotopic composition of the snow, the water vapor
455 in the air and recrystallization due to temperature gradients. Our results demonstrate that
456 recrystallization and bulk mass exchange must be incorporated into future models of
457 snow and firn evolution. Further studies are required on the influence of temperature
458 and airflow as well as snow microstructure on the mass transfer phenomena for
459 validating the implementation of stable water isotopes in snow models.

460

461

462 **Acknowledgements**

463 The Swiss National Science Foundation granted financial support under project Nr.
464 200020-146540. H.C. Steen-Larsen was supported by the AXA Research Fund. The
465 authors thank K. Fujita, E. D. Waddington and an anonymous reviewer for the
466 suggestions and critical review. M. Jaggi, S. Grimm, A. Schlumpf, and S. Berben gave
467 technical support. The data for this paper are available by contacting the corresponding
468 author.

470 **References**

- 471 Albert M. R. and Hardy J. P.: Ventilation experiments in a seasonal snow cover, in
472 Biogeochemistry of Seasonally Snow-Covered Catchments, IAHS Publ. 228, edited
473 by K. A. Tonnessen, M. W. Williams, and M. Tranter, 41–49, IAHS Press,
474 Wallingford, UK, 1995.
- 475 Calonne N., Geindreau C., Flin F., Morin S., Lesaffre B., Rolland du Roscoat S., and
476 Charrier P.: 3-D image-based numerical computations of snow permeability: links
477 to specific surface area, density, and microstructural anisotropy, *The Cryosphere*, 6,
478 939-951, 2012.
- 479 Casado M., Landais A., Masson-Delmotte V., Genthon C., Kerstel E., Kassi S., Arnaud
480 L., Picard G., Prie F., Cattani O., Steen-Larsen H. C., Vignon E., and Cermak P.:
481 Continuous measurements of isotopic composition of water vapour on the East
482 Antarctic Plateau, *Atmos. Chem. Phys. Discuss.*, doi:10.5194/acp-2016-8, in
483 review, 2016.
- 484 Ciais P., and Jouzel J.: Deuterium and oxygen 18 in precipitation: Isotopic model,
485 including mixed-cloud processes, *Journal of Geophysical Research*, 99, 16793–
486 16803, doi:10.1029/94JD00412, 1994.
- 487 Colbeck S. C.: Air movement in snow due to windpumping, *Journal of Glaciology*, 35,
488 209–213, 1989.
- 489 Craig H. and Gordon L. I.: Deuterium and oxygen 18 variations in the ocean and marine
490 atmosphere, In *proc. Stable Isotopes in Oceanographic Studies and*
491 *Paleotemperatures*, (ed. E. Toniorgi), Spoleto, Italy, 9–130, 1964.

492 Cuffey K. M. and Steig E. J.: Isotopic diffusion in polar firn: Implications for
493 interpretation of seasonal climate parameters in ice-core records, with emphasis on
494 central Greenland, *Journal of Glaciology*, 44, 273–284, 1998.

495 Cuffey K. M., Alley R. B., Grootes P. M., Bolzan J. M., and Anandakrishnan S.:
496 Calibration of the Delta-O-18 isotopic paleothermometer for central Greenland,
497 using borehole temperatures, *Journal of Glaciology*, 40, 341–349, 1994.

498 Dansgaard W.: Stable isotopes in precipitation, *Tellus*, 16, 436–468, 1964.

499 Ebner P. P., Grimm S., Schneebeli M., and Steinfeld A.: An instrumented sample holder
500 for time-lapse micro-tomography measurements of snow under advective
501 conditions, *Geoscientific Instrumentation Methods and Data Systems*, 3, 179–185,
502 doi:10.5194/gi-3-179-2014, 2014.

503 Ebner P. P., Schneebeli M., and Steinfeld A. Tomography-based observation of
504 isothermal snow metamorphism under advective conditions, *The Cryosphere*, 9,
505 1363–1371, 2015a.

506 Ebner P. P., Andreoli C., Schneebeli M., and Steinfeld A.: Tomography-based
507 characterization of ice-air interface dynamics of temperature gradient snow
508 metamorphism under advective conditions, *Journal of Geophysical Research*,
509 *Journal of Geophysical Research Earth Surface*, 120, doi:10.1002/2015JF003648,
510 2015b.

511 Ebner P. P., Schneebeli M., and Steinfeld A.: Metamorphism during temperature
512 gradient with undersaturated advective airflow in a snow sample, *The Cryosphere*,
513 10, 791-797, 2016.

514 EPICA Members: Eight glacial cycles from an Antarctic ice core, *Nature*, 429, 623–
515 628, doi:10.1038/nature02599, 2004.

516 Gjessing Y. T.: The filtering effect of snow, in: *Isotopes and Impurities in Snow and Ice*
517 *Symposium*, edited by: Oeschger, H., Ambach, W., Junge, C. E., Lorius, C., and
518 Serebryanny, L., IASHAISH Publication, Dorking, 118, 199–203, 1977.

519 Grootes P. M., Steig E., and Stuiver M.: Taylor Ice Dome study 1993-1994: An ice core
520 to bedrock, *Antarctic Journal U.S.*, 29, 79–81, 1994.

521 Fisher D. A., Koerner R. M., Paterson W. S. B., Dansgaard W., Gundestrup N., and
522 Reeh N.: Effect of wind scouring on climatic records from ice-core oxygen-isotope
523 profiles, *Nature*, 301, 205–209, doi:10.1038/301205a0, 1983.

524 Fisher D. A. and Koerner R.: The effect of wind on d(18O) and accumulation given an
525 inferred record of seasonal d amplitude from the Agassiz ice cap, Ellesmere island,
526 Canada, *Annals of Glaciology*, 10, 34–37, 1988.

527 Fisher D. A. and Koerner R.: Signal and noise in four ice-core records from the Agassiz
528 ice cap, Ellesmere Island, Canada: Details of the last millennium for stable
529 isotopes, melt and solid conductivity, *The Holocene*, 4, 113–120,
530 doi:10.1177/095968369400400201, 1994.

531 Friedman I., Benson C., and Gleason J.: Isotopic changes during snow metamorphism,
532 in *Stable Isotope Geochemistry: A Tribute to Samuel Epstein*, edited by J. R.
533 O'Neill and I. R. Kaplan, pp. 211–221, Geochemical Society, Washington, D. C.,
534 1991.

535 Haussener S., Gergely M., Schneebeli M., and Steinfeld A.: Determination of the
536 macroscopic optical properties of snow based on exact morphology and direct pore-
537 level heat transfer modeling, *Journal of Geophysical Research*, 117, 1–20,
538 doi:10.1029/2012JF002332, 2012.

539 He H. and Smith R. B.: An advective-diffusive isotopic evaporation-condensation
540 model, *Journal of Geophysical Research*, 104, 18619-18630,
541 doi:10.1029/1999JD900335, 1999.

542 Helsen M. M., van de Wal R. S. W., van den Broeke M. R., van As D., Meijer H. A. J.,
543 and Reijmer C. H.: Oxygen isotope variability in snow from western Dronning
544 Maud Land, Antarctica and its relation to temperature, *Tellus*, 57, 423–435, 2005.

545 Helsen M. M., van de Wal R. S. W., van den Broeke M. R., Masson-Delmotte V.,
546 Meijer H. A. J., Scheele M. P., and Werner M., Modeling the isotopic composition
547 of Antarctic snow using backward trajectories: Simulation of snow pit records,
548 *Journal of Geophysical Research*, 111, doi:10.1029/2005JD006524, 2006.

549 Helsen M. M., van de Wal R. S. W., and van den Broeke M. R.: The isotopic
550 composition of present-day Antarctic snow in a Lagrangian simulation, *Journal of*
551 *Climate*, 20, 739–756, 2007.

552 Hendricks M. B., DePaolo D. J., and Cohen R. C.: Space and time variation of $\delta^{18}\text{O}$ and
553 δD in precipitation: Can paleotemperature be estimated from ice cores?, *Global*
554 *Biogeochemical Cycles*, 14, 851–861, doi:10.1029/1999GB001198, 2000.

555 Horita J., Rozanski K., and Cohen S.: Isotope effects in the evaporation of water: a
556 status report of the Craig-Gordon model, *Isotopes in Environmental Health Studies*,
557 44, 23-49, doi:10.1080/10256010801887174, 2008.

558 Hoshina Y., Fujita K., Nakazawa F., Iizuka Y., Miyake T., Hirabayashi M., Kuramoto
559 T., Fujita S., and Motoyama H.: Effect of accumulation rate on water stable
560 isotopes of near-surface snow in inland Antarctica. *Journal of Geophysical*
561 *Research - Atmospheres*, 119(1), 274-283. doi:10.1002/2013JD020771, 2014.

562 Hoshina Y., Fujita K., Iizuka Y., Motoyama H.: Inconsistent relations among major ions
563 and water stable isotopes in Antarctica snow under different accumulation
564 environments. *Polar Science*, 10, doi:10.1016/j.polar.2015.12.003, 2016.

565 Johnsen S. J.: Stable isotope homogenization of polar firn and ice, in *Isotopes and*
566 *Impurities in Snow and Ice*, Proceeding of the Grenoble Symposium,
567 August/September 1975, 210–219, IAHS AISH Publication, 118, Grenoble, France,
568 1997.

569 Johnsen S. J., Clausen H. B., Cuffey K. M., Hoffman G., Schwander J., and Creyts T.:
570 Diffusion of stable isotopes in polar firn and ice: The isotope effect in firn
571 diffusion, in *Physics of Ice Core Records*, edited by T. Hondoh, 121–140,
572 Hokkaido University Press, Sapporo, Japan, 200.

573 Johnsen S. J., Dahl-Jensen D., Gundestrup N., Steffensen J. P., Clausen H. B., Miller
574 H., Masson-Delmotte V., Sveinbjörnsdóttir A. E., and White J.: Oxygen isotope
575 and palaeotemperature records from six Greenland ice-core stations: Camp
576 Century, DYE-3, GRIP, GISP2, Renland and NorthGRIP, *Journal of Quaternary*
577 *Science*, 16, 299–307, doi:10.1002/jqs.622, 2001.

578 Jouzel J. and Merlivat L.: Deuterium and oxygen 18 in precipitation: Modeling of the
579 isotopic effects during snow formation, *Journal of Geophysical Research*, 89,
580 11749–11757, doi:10.1029/JD089iD07p11749, 1984.

581 Jouzel J., Merlivat L., Petit J. R., and Lorius C.: Climatic information over the last
582 century deduced from a detailed isotopic record in the South Pole snow, *Journal of*
583 *Geophysical Research*, 88, 2693–2703, doi:10.1029/JC088iC04p02693, 1983.

584 Jouzel J., et al.: Validity of the temperature reconstruction from water isotopes in ice
585 cores, *Journal of Geophysical Research*, 102, 26471–26487,
586 doi:10.1029/97JC01283, 1997.

587 Jouzel J., Vimeux F., Caillon N., Delaygue G., Hoffman G., Masson-Delmotte V., and
588 Parrenin F.: Magnitude of isotope/temperature scaling for interpretation of central
589 Antarctic ice cores, *Journal of Geophysical Research*, 108, 1–6,
590 doi:10.1029/2002JD002677, 2003.

591 Kaempfer T. U., and Schneebeli M. Observation of isothermal metamorphism of new
592 snow and interpretation as a sintering process, *Journal of Geophysical Research*,
593 112(D24), 1–10, doi:10.1029/2007JD009047, 2007.

594 Krinner G. and Werner M.: Impact of precipitation seasonality changes on isotopic
595 signals in polar ice cores: A multi-model analysis, *Earth and Planetary Science*
596 *Letters*, 216, 525–538, doi:10.1016/S0012-821X(03)00550-8, 2003.

597 Lorius C., Merlivat L., Jouzel J., and Pourchet M.: A 30,000-yr isotope climatic record
598 from Antarctica ice, *Nature*, 280, 644–648, doi:10.1038/280644a0, 1979.

599 Löwe H., Spiegel J. K., and Schneebeli M.: Interfacial and structural relaxations of
600 snow under isothermal conditions, *Journal of Glaciology*, 57, 499-510,
601 doi:10.3189/002214311796905569, 2011.

602 Masson-Delmotte V., Steen-Larsen H. C., Ortega P., Swingedouw D., Popp T., Vinther
603 B. M., Oerter H., Sveinbjornsdottir A. E., Gudlaugsdottir H., Box J. E., Falourd S.,
604 Fettweis X., Gallee H., Garnier E., Jouzel J., Landais A., Minster B., Paradis N.,
605 Orsi A., Risi C., Werner M., and White J. W. C.: Recent changes in north-west
606 Greenland climate documented by NEEM shallow ice core data and simulations,
607 and implications for past temperature reconstructions, *The Cryosphere*, 9, 1481-
608 1504, doi:10.5194/tc-9-1481-2015, 2015.

609 Merlivat L. and Jouzel J.: Global climatic interpretation of the deuterium-oxygen 18
610 relationship for precipitation, *Journal of Geophysical Research*, 84, 5029–5033,
611 doi:10.1029/JC084iC08p05029, 1979.

612 Neumann T. A.: Effects of firn ventilation on geochemistry of polar snow, PhD thesis,
613 University of Washington, Washington, USA, 2003.

614 Neumann T. A. and Waddington E. D.: Effects of firn ventilation on isotopic exchange,
615 Journal of Glaciology, 50, 183–194, 2004.

616 Neumann T. A., Albert M. R., Lomonaco R., Engel C., Courville Z., and Perron F.:
617 Experimental determination of snow sublimation rate and stable-isotopic exchange,
618 Annals of Glaciology, 49, 1–6, doi:10.3189/172756408787814825, 2008.

619 Otsu N.: A Threshold Selection Method from Gray-Level Histograms, IEEE
620 Transactions on Systems Man and Cybernetics, 9, 62–66, 1979.

621 Penna, D., Stenni, B., Šanda, M., Wrede, S., Bogaard, T. A., Michelini, M., et al.:
622 Technical Note: Evaluation of between-sample memory effects in the analysis of
623 $\delta^2\text{H}$ and $\delta^{18}\text{O}$ of water samples measured by laser spectroscopes. Hydrology and
624 Earth System Sciences, 16(10), 3925–3933. [http://doi.org/10.5194/hess-16-3925-](http://doi.org/10.5194/hess-16-3925-2012)
625 [2012](http://doi.org/10.5194/hess-16-3925-2012), 2012.

626 Persson A., Langen P. L., Ditlevsen P., and Vinther B. M.: The influence of
627 precipitation weighting on interannual variability of stable water isotopes in
628 Greenland, Journal of Geophysical Research – Atmosphere, 116, 1-13,
629 doi:10.1029/2010JD015517, 2011.

630 Petit J. R., et al.: Climate and atmospheric history of the past 420,000 years from the
631 Vostok ice core, Antarctica, Nature, 399, 429–436, doi:10.1038/20859, 1999.

632 Pinzer B. R. and Schneebeli M.: Snow metamorphism under alternating temperature
633 gradients: Morphology and recrystallization in surface snow, Geophysical Research
634 Letters, 36, doi:10.1029/2009GL039618, 2009.

635 Pinzer B. R., Schneebeli M., and Kaempfer T. U.: Vapor flux and recrystallization
636 during dry snow metamorphism under a steady temperature gradient as observed by

637 time-lapse microtomography, *The Cryosphere*, 6, 1141–1155, doi:10.5194/tc-6-
638 1141-2012, 2012.

639 Ramseier R. O: Self-diffusion of tritium in natural and synthetic ice monocrystals,
640 *Journal of Applied Physics*, 38, 2553-2556, 1967.

641 Ritter F., Steen-Larsen H. C., Werner M., Masson-Delmotte V., Orsi A., Behrens M.,
642 Birnbaum G., Freitag J., Risi C., and Kipfstuhl S.: Isotopic exchange on the diurnal
643 scale between near-surface snow and lower atmospheric water vapor at Kohnen
644 station, East Antarctica, *The Cryosphere Discussion*, doi:10.5194/tc-2016-4, in
645 review, 2016.

646 Schleef S., Jaggi M., Löwe H., and Schneebeli M.: Instruments and Methods: An
647 improved machine to produce nature-identical snow in the laboratory, *Journal of*
648 *Glaciology*, 60, 94–102, 2014.

649 Sjolte J., Hoffmann G., Johnsen S. J., Vinther B. M., Masson-Delmotte V., and Sturm
650 C.: Modeling the water isotopes in Greenland precipitation 1959-2001 with the
651 meso-scale model remo-iso, *Journal of Geophysical Research*, 116, 1-22,
652 doi:10.1029/2010JD015287, 2011.

653 Sokratov S. A. and Golubev V. N.: Snow isotopic content change by sublimation.
654 *Journal of Glaciology*, 55(193), 823-828, doi:10.3189/002214309790152456, 2009.

655 Steen-Larsen H. C., Masson-Delmotte V., Sjolte J., Johnsen S. J., Vinther B. M., Breon
656 F. M., Clausen H. B., Dahl-Jensen D., Falourd S., Fettweis X., Gallee H., Jouzel J.,
657 Kageyama M., Lerche H., Minster B., Picard G., Punge H. J., Risi C.,
658 Salas D., Schwander J., Steffen K., Sveinbjornsdottir A. E., Svensson A., and
659 White J.: Understanding the climatic signal in the water stable isotope records from
660 the neem shallow firn/ice cores in northwest Greenland, *Journal of Geophysical*
661 *Research - Atmosphere*, 116, 1–20, doi:10.1029/2010JD014311, 2011.

662 Steen-Larsen H. C., Johnsen S. J., Masson-Delmotte V., Stenni B., Risi C., Sodemann
663 H., Balslev-Clausen D., Blunier T., Dahl-Jensen D., Ellehøj M. D., Falourd S.,
664 Grindsted A., Gkinis V., Jouzel J., Popp T., Sheldon S., Simonsen S. B., Sjolte J.,
665 Steffensen J. P., Sperlich P., Sveinbjörnsdóttir A. E., Vinther B. M., and Whiste J.
666 W. C.: Continuous monitoring of summer surface water vapor isotopic composition
667 above the Greenland Ice Sheet, *Atmospheric Chemistry and Physics*, 13, 4815–
668 4828, doi: 10.5194/acp-13-4815-2013, 2013.

669 Steen-Larsen H. C., Masson-Delmotte V., Hirabayashi M., Winkler R., Satow K., Prié
670 F., Bayou N., Brun E., Cuffey K. M., Dahl-Jensen D., Dumont M., Guillevic M.,
671 Kipfstuhl S., Landais A., Popp T., Risi C., Steffen K., Stenni B., and
672 Sveinbjörnsdóttir A. E.: What controls the isotopic composition of Greenland
673 surface snow?, *Climate of the Past*, 10, 377–392, doi:10.5194/cp-10-377-2014.,
674 2014a.

675 Steen-Larsen H. C., Sveinbjörnsdóttir A. E., Peters A. J., Masson-Delmotte V.,
676 Guishard M. P., Hsiao G., Jouzel J., Noone D., Warren J. K., and White J. W. C.:
677 Climatic controls on water vapor deuterium excess in the marine boundary layer of
678 the North Atlantic based on 500 days of in situ, continuous measurements,
679 *Atmospheric Chemistry and Physics*, 14, 7741-7756, doi:10.5194/acp-14-7741-
680 2014., 2014b.

681 Sturm M. and Johnson J. B.: Natural convection in the subarctic snow cover, *Journal of*
682 *Geophysical Research*, 96, 11657–11671, doi:10.1029/91JB00895, 1991.

683 Town M. S., Warren S. G., Walden V. P., and Waddington E. D.: Effect of atmospheric
684 water vapor on modification of stable isotopes in near-surface snow on ice sheets,
685 *Journal of Geophysical Research-Atmosphere*, 113, 1-16,
686 doi:10.1029/2008JD009852, 2008.

687 Van der Wel G., Fischer H., Oerter H., Meyer H., and Meijer H. A. J.: Estimation and
688 calibration of the water isotope differential diffusion length in ice core records, *The*
689 *Cryosphere Discussion*, 9, 927-973, doi:10.5194/tc-9-1601-2015, 2015

690 Waddington E. D., Cunningham J., and Harder S. L.: The effects of snow ventilation on
691 chemical concentrations, in: *Chemical Exchange Between the Atmosphere and*
692 *Polar Snow*, edited by: Wolff, E. W. and Bales, R. C., Springer, Berlin, NATO ASI
693 Series, 43, 403–452, 1996.

694 Waddington E. D., Steig E. J., and Neumann T. A.: Using characteristic times to assess
695 whether stable isotopes in polar snow can be reversibly deposited. *Annals of*
696 *Glaciology*, 35, 118–124, doi:10.3189/172756402781817004, 2002.

697 Werner M., Langebroek P. M., Carlsen T., Herold M., and Lohmann G.: Stable water
698 isotopes in the ECHAM5 general circulation model: Toward high-resolution
699 isotope modeling on a global scale, *Journal of Geophysical Research Atmosphere*,
700 116, D15109, doi:10.1029/2011JD015681, 2011.

701 White J. W., Barlow L. K., Fisher D., Grootes P., Jouzel J., Johnsen S. J., Stuiver M.,
702 and Clausen H.: The climate signal in the stable isotopes of snow from Summit,
703 Greenland: Results of comparisons with modern climate observations, *Journal of*
704 *Geophysical Research*, 102, 26425–26439, doi:10.1029/97JC00162, 1997.

705 Zermatten E., Schneebeli M., Arakawa H., and Steinfeld A.: Tomography-based
706 determination of porosity, specific area and permeability of snow and comparison
707 with measurements, *Cold Regions Science and Technology*, 97, 33–40,
708 doi:10.1016/j.coldregions.2013.09.013, 2014.

709

710

711 **Table 1:** Morphological properties and flow characteristics of the experimental runs:
712 **μ CT measured** snow density (ρ), porosity (ε), specific surface area per unit mass (SSA),
713 mean pore space diameter (d_{mean}), superficial velocity in snow (u_D), corresponding
714 Reynolds number ($\text{Re} = d_{\text{mean}} \cdot u_D / \nu_{\text{air}}$), average inlet temperature of the humidifier and
715 at the inlet ($T_{\text{in,mean}}$), average outlet temperature at the outlet ($T_{\text{out,mean}}$), and average
716 temperature gradient (∇T_{ave}). Experiment (1) corresponds to the isothermal conditions;
717 Experiment (2) to air warming; and Experiment (3) to air cooling in the snow sample.
718

	ρ kg m ⁻³	ε –	SSA m ² kg ⁻¹	d_{mean} mm	u_D m s ⁻¹	Re –	$T_{\text{in,mean}}$ °C	$T_{\text{out,mean}}$ °C	∇T_{ave} K m ⁻¹
Experiment (1)	202	0.78	28	0.39	0.03	0.76	-15.5	-15.5	–
Experiment (2)	202	0.78	30	0.36	0.03	0.70	-15.4	-14.0	+47
Experiment (3)	220	0.76	27	0.37	0.031	0.74	-12.3	-14.1	-60

719

720 **Table 2:** $\delta^{18}\text{O}$ in the vapor in the humidifier ($\delta^{18}\text{O}_{\text{hum}}$) and of the snow in the sample
721 holder ($\delta^{18}\text{O}_s$) at the beginning ($t = 0$) and end ($t = \text{end}$) of each experiment and the final
722 $\delta^{18}\text{O}$ content of the snow in the sample holder at the inlet ($z = 0$ mm) and outlet ($z = 30$
723 mm). Experiment (1) corresponds to the isothermal conditions; Experiment (2) to air
724 warming; and Experiment (3) to air cooling in the snow sample.

725

	$\delta^{18}\text{O}_{\text{hum}}$		$\delta^{18}\text{O}_{s, t=0}$	$\delta^{18}\text{O}_{s, t=\text{end}}$	
	%o			%o	
	$t = 0$	$t = \text{end}$		$z = 0$ mm	$z = 30$ mm
Experiment (1)	-68.2	-67.5	-10.97	-17.75	-15.72
Experiment (2)	-66.3	-66.1	-11.94	-19.60	-16.60
Experiment (3)	-62.8	-62.2	-10.44	-25.53	-15.00

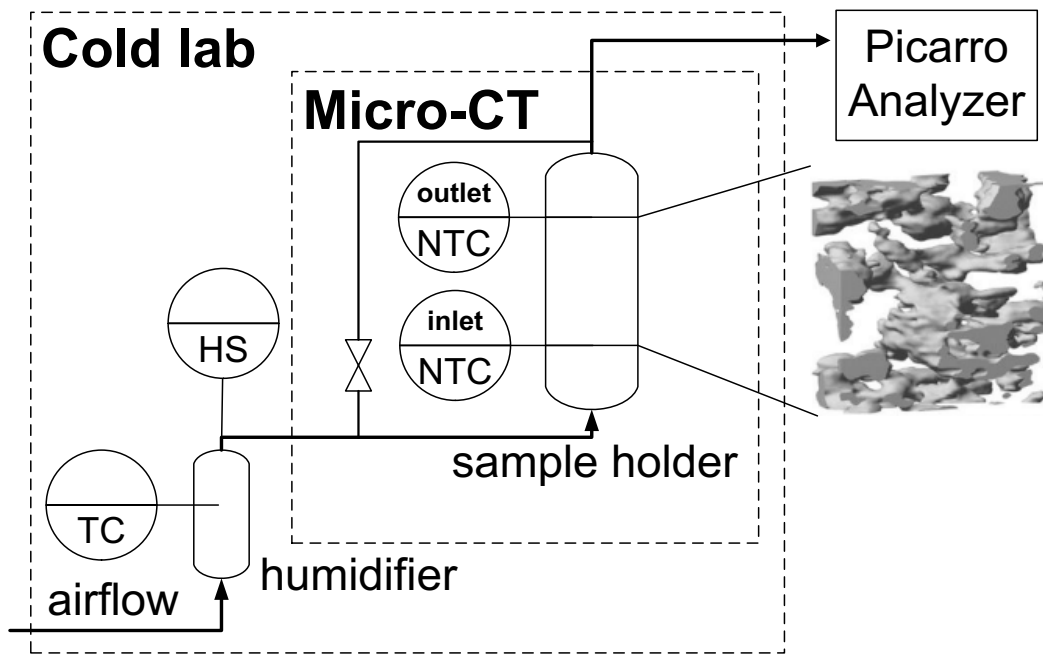
726

727 **Figure captions**

728 **Fig. 1.** Schematic of the experimental setup. A thermocouple (TC) and a humidity
729 sensor (HS) inside the humidifier measured the the mean temperature and
730 humidity of the airflow. Two thermistors (NTC) close to the snow surface
731 measured the inlet and outlet temperature of the airflow (Ebner et al., 2014).
732 The Picarro Analyzer measured the isotopic composition $\delta^{18}\text{O}$ of the outlet
733 flow. Inset: 3D structure of $110 \times 42 \times 110$ voxels ($2 \times 0.75 \times 2 \text{ mm}^3$)
734 obtained by the μCT .

735 **Fig. 2.** Temporal isotopic composition of $\delta^{18}\text{O}$ of the outflow for each of the
736 experimental runs. The spikes in the $\delta^{18}\text{O}$ were due to small temperature
737 changes in the cold laboratory (Ebner et al., 2014). Exp. (1) corresponds to
738 the isothermal conditions; Exp. (2) to air warming; and Exp. (3) to air
739 cooling in the snow sample. The higher the recrystallization rate of the snow
740 the slower the adaption of $\delta^{18}\text{O}$ of the outlet air to the inlet air. The
741 illustration in the lower right corner shows the relation between $\delta^{18}\text{O}$ of the
742 initial snow, inlet, and outlet of the air.

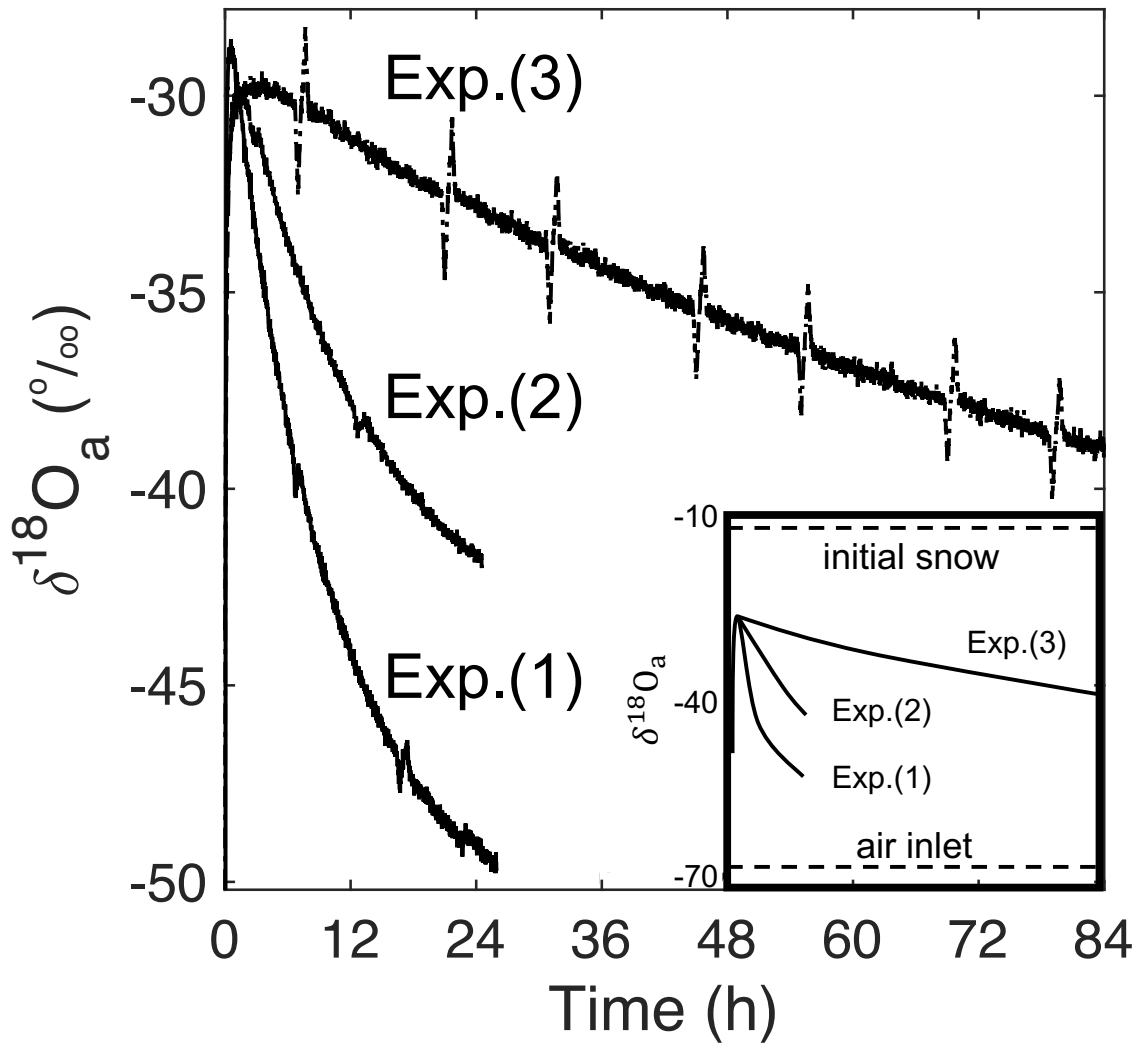
743 **Fig. 3.** Spatial isotopic composition of $\delta^{18}\text{O}$ of the snow sample at the beginning (t
744 $= 0$) and at the end ($t = \text{end}$) for each experiment. The air entered at $z = 0$
745 mm and exited at $z = 30$ mm. Exp. (1) corresponds to the isothermal
746 conditions; Exp. (2) to air warming; and Exp. (3) to air cooling in the snow
747 sample.



748

749

Fig. 1

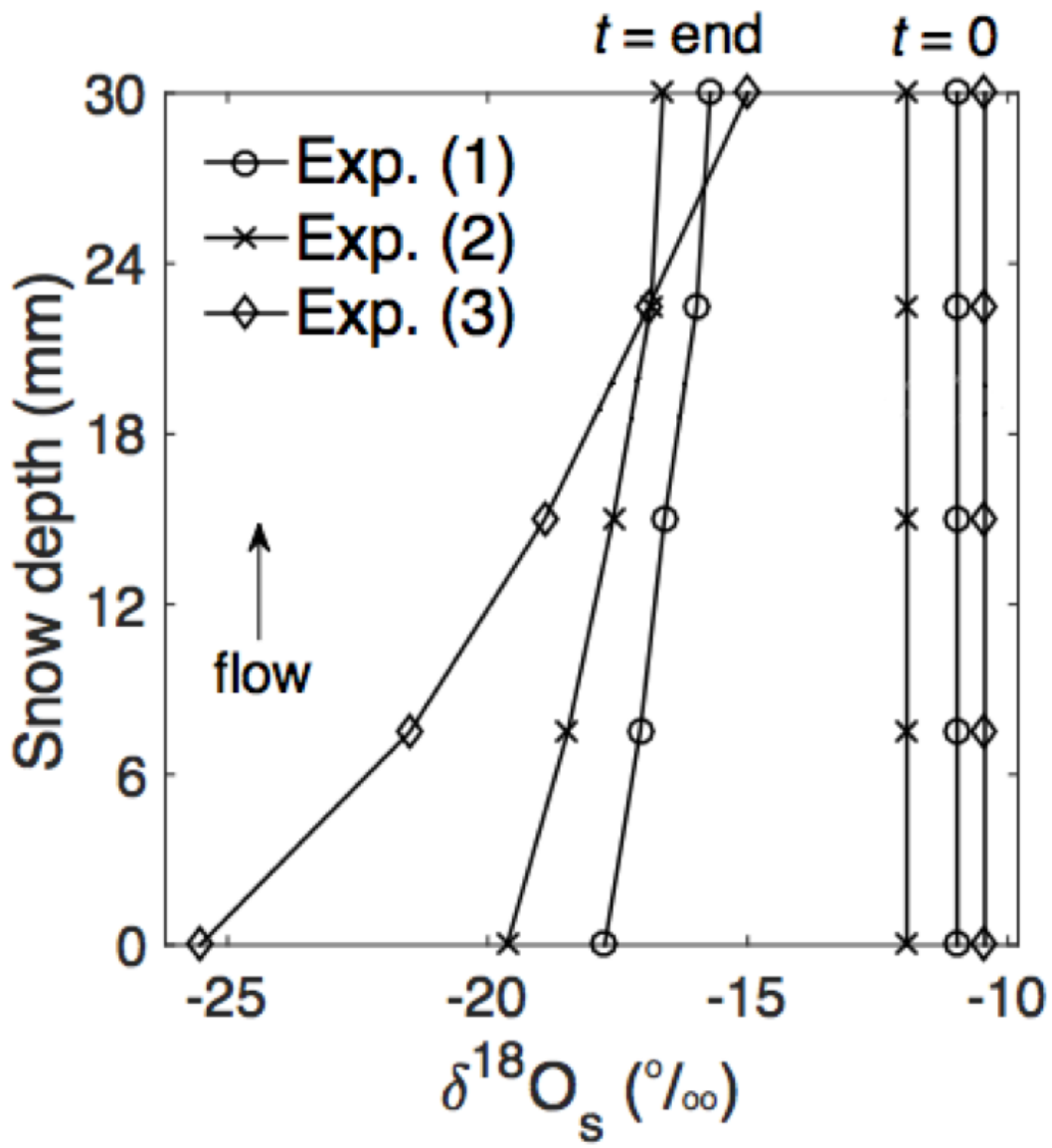


750

751

752

Fig. 2



753

754

Fig. 3